Journal Name

ARTICLE TYPE

Cite this: DOI: 10.1039/xxxxxxxxxx

Supplemental material of: Charge polarization, local electroneutrality breakdown and eddy formation due to electroosmosis in varying-section channels†

Mauro Chinappi,*[a] Paolo Malgaretti,*[b]

Received Date
Accepted Date

DOI: 10.1039/xxxxxxxxxx

www.rsc.org/journalname

1 Ion and electroosmotic currents

Here, we discuss the dependence of ionic and electroosmotic currents on the applied voltage. Figures S1.a and S1.b show the electro-osmotic flow Q and the ionic current I as a function of the applied electrostatic potential drop $\Delta V = L_x E_x$ along with the predictions of Poisson-Nernst-Plank (PNP) theory presented in [1]. Both panels of Fig S1 show a significant mismatch between the numerical results (symbols) and the PNP model (dashed lines). Interestingly the mismatch increases upon increasing the salt concentration, i.e. decreasing the Debye length. As discussed in the main text, the effect of the slip on the walls of the channel increases as the ratio L_s/λ_D where L_s is the so-called slip length and it captures the magnitude of the slip. In this perspective, Fig.S1.a makes us speculate that the mismatch between the numerical results and the PNP model is due to the partial slip of the fluid on the channel walls. Indeed, for high concentration (low λ_D), the MD electro-osmotic flux (blue triangles) is significantly larger than the PNP prediction (dashed blue line). The partial slip can also explain the mismatch shown in Fig.S1.b. While in a flat channel an enhancement of the volumetric fluid flow Q leads to an increased electric current (see Ref. [2]) the situation is different in the case of a corrugated channel. Indeed, in the latter case the K^+ ions have to overcome a potential barrier at the channel bottleneck whereas Cl^- can move along the channel walls at almost constant potential. Therefore the enhanced Q will reduce the magnitude of the effective barrier that K^+ have to overcome. Since the flow is quite sensitive to the high of the barrier (for very large barrier the time scales *exponentially* with the high of the barrier) the enhancement of Q will be more beneficial to the flow of K^+ as compared to the gain for Cl^-. Since the electric current is defined as $I = J_K - J_{Cl}$ the enhancement of Q leads to a hampered electric current, i.e. the electric currents from MD (symbols) are smaller than the PNP predictions (dashed lines), in particular for larger ionic concentrations.

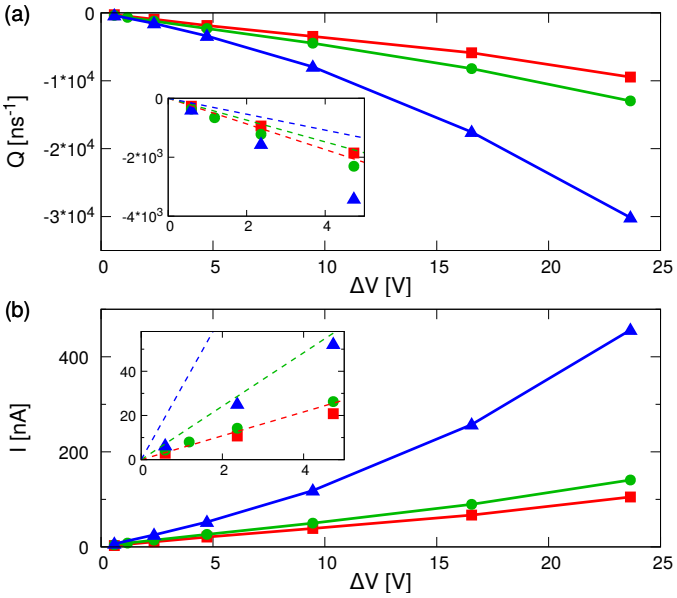

Fig. S1 Electrolyte transport. a): Electro-osmotic flux Q expressed in water molecules per ns as function of ΔV. Different colors stand for different concentrations, namely $\rho_0 = 0.3$M (green circles) $\rho_0 = 1$M (red squares) and $\rho_0 = 3$M (blue triangles). b): Ionic current for different electrostatic potential drops ΔV. Ionic concentrations are color-coded as in panel a). The insets of both panels show the PNP prediction (dashed lines) in the low voltage regime.

2 Methods

System set-up and equilibration. The system is constituted by a KCl water solution confined by two solid walls. The solid

[a] *Dipartimento di Ingegneria Industriale, Università di Roma Tor Vergata, via del Politecnico 1, 00133 Roma, Italia; E-mail: mauro.chinappi@uniroma2.it*
[b] *Max-Planck-Institut für Intelligente Systeme, Heisenbergstr. 3, D-70569 Stuttgart, Germany; E-mail: malgaretti@is.mpg.de*
[c] *IV Institute for Theoretical Physics, University of Stuttgart, Pfaffenwaldring 57, 70569 Stuttgart, Germany*

walls are formed by atoms arranged in a face centered cubic (fcc) structure with lattice side $a = 4.92$ Å. The mass of each atom is $m_w = 70\ a.m.u.$ and they interact via Lennard-Jones potential with potential well depth $\varepsilon_w = 0.152$ Kcal/mol) and van der Waals radius $\sigma_w = 3.15$ Å. The curved walls are obtained by solid slabs cut parallel to 111 planes of the fcc solid. The two slabs are then bend to follow the prescribed channel shape with a proper change of the z-coordinate. Each atom exposed to the liquid has a charge q_w.

Water molecules and ions at a molar concentration ρ_0 are added using VMD[3]. In particular, indicated with N_{Cl^-} and N_{K^+} the number of Chloride and Potassium ions, we have $N_{Cl^-} = 1749$ and $N_{K^+} = 789$ for $\rho_0 = 0.3M$, $N_{Cl^-} = 3327$ and $N_{K^+} = 2367$ for $\rho_0 = 1M$, and $N_{Cl^-} = 8062$ and $N_{K^+} = 7102$ for $\rho_0 = 3M$. In each case, $N_{Cl^-} - N_{K^+} = 960$. Since 960e is the total charge on the walls, the total charge of the system is zero.

All MD simulations are performed using NAMD software[4] by implementing periodic boundary conditions being $L_x = 836.6$ Å, $L_y = 60.37$ Å and $L_z = 200$ Å the box sizes. L_x and L_y are dictated by the size of solid walls while L_z is arbitrary set to 200 Å to avoid non-bonded interactions among the different images along the z-axes. The total number of atoms is ∼400 000. A snapshot of the system is reported in figure 1.b. Particle mesh Ewalds (PME) summation method was employed for the electrostatics[5]. TIP3P model[6] was employed for water while CHARMM36 force field[7,8] with NBFIX corrections is used for the ions[9]. More accurate water models are available, see e.g. the TIP4P_2005[10] often used for nanofluidics[11,12]. However, these models are much more computational demanding than TIP3P, hence, in this work, beside the well known limitations of TIP3P (e.g. the viscosity is lower than the experimental value) we preferred TIP3P since it allowed us to run longer simulations and to partially reduce the statistical error.

Walls atoms are constrained at their initial position by harmonic springs (spring constant $k = 10$ Kcal/(mol Å^2)). A first 0.8 ns NVT simulations ($T = 310$K, time step 2 fs) was run and pressure is estimated from the average force acting on the walls. The distance between the upper and lower wall is then gradually reduced and further 0.8 ns simulations are run until the pressure reached a value close to 1 atm.

Production runs. As common in the MD studies on ionic and electroosmotic transport, a homogeneous and constant external electric field $\mathbf{E} = (E_x, 0, 0)$ is applied to the whole system[13–15]. Snapshots are acquired every $\Delta t = 2$ps.

The water velocity field in the x,z plane is calculated as follows. The velocity $\mathbf{v_i}$ of the i-th water molecule is estimated as $\mathbf{v}_i = [\mathbf{x}_i(t+\Delta t) - \mathbf{x_i}(t)]/\Delta t$ where $\mathbf{x_i}$ is the position of the oxygen atom of the i-th water molecule. The mean velocity of each particle $\mathbf{v_i}$ is associated to the point $\hat{\mathbf{x}}_i = [\mathbf{x}_i(t+\Delta t) + \mathbf{x}_i(t)]/2$. The value of the velocity field $\mathbf{u}$ in a given point $\mathbf{x}$ is hence calculated as the mean of the velocities of the particles in the neighborhood of $\mathbf{x}$, i.e. the molecule for which $\hat{\mathbf{x}}_\mathbf{i}$ belongs to a region $[x - \Delta x/2, x + \Delta x/2] \cap [z - \Delta z/2, z + \Delta z/2]$. The production runs span in a range of $40 - 90$ ns with longer simulations used for smaller forcing and lower ionic concentration.

References

1 P. Malgaretti, I. Pagonabarraga and J. M. Rubi, *Phys. Rev. Lett*, 2014, **113**, 128301.

2 H. Bruus, *Theoretical microfluidics*, Oxford university press Oxford, 2008, vol. 18.

3 W. Humphrey, A. Dalke and K. Schulten, 1996, **14**, 33.

4 J. C. Phillips, R. Braun, W. Wang, J. Gumbart, E. Tajkhorshid, E. Villa, C. Chipot, R. D. Skeel, L. Kale and K. Schulten, 2005, **26**, 1781.

5 P. F. Batcho, D. A. Case and T. Schlick, 2001, **115**, 4003.

6 W. L. Jorgensen, J. Chandrasekhar, J. D. Madura, R. W. Impey and M. L. Klein, 1983, **79**, 926.

7 B. R. Brooks, C. L. Brooks, A. D. MacKerell, L. Nilsson, R. J. Petrella, B. Roux, Y. Won, G. Archontis, C. Bartels, S. Boresch and o. others, *Journal of computational chemistry*, 2009, **30**, 1545.

8 K. Vanommeslaeghe and A. D. MacKerell Jr, 2012, **52**, 3144.

9 Y. Luo and B. Roux, *The Journal of Physical Chemistry Letters*, 2009, **1**, 183.

10 J. L. Abascal and C. Vega, *The Journal of chemical physics*, 2005, **123**, 234505.

11 D. Gentili, G. Bolognesi, A. Giacomello, M. Chinappi and C. Casciola, *Microfluidics and nanofluidics*, 2014, **16**, 1009.

12 A. Tinti, A. Giacomello, Y. Grosu and C. M. Casciola, *Proceedings of the National Academy of Sciences*, 2017, 201714796.

13 A. Aksimentiev and K. Schulten, 2005, **88**, 3745.

14 J. Wilson, L. Sloman, Z. He and A. Aksimentiev, *Advanced functional materials*, 2016, **26**, 4830.

15 E. L. Bonome, F. Cecconi and M. Chinappi, *Microfluidics and Nanofluidics*, 2017, **21**, 96.